Use of tritium to predict soluble pollutants transport in Ebro river waters (Spain)

Ll. Pujol* and J.A. Sanchez-Cabeza

Departament de Física, Universitat Autònoma de Barcelona, ES-08193 Bellaterra, Barcelona, Spain

* Corresponding author, tel: +3491-335.72.28, fax: +3491-335.72.67, e-mail: Luis.Pujol@cedex.es

Abstract

The Ebro river, in Northeast Spain, discharges into the Mediterranean Sea after flowing through several large cities and agricultural, mining and industrial areas. The Ascó nuclear power plant (NPP) is located in its lower section and comprises two pressurised-water reactor (PWR) units, from which low-level liquid radioactive waste is released to river waters under authority control. Tritium routinely released by the NPP was used as a radiotracer to determine the longitudinal dispersion coefficient and velocity of the river waters. Several field experiments, in co-ordination with the NPP, were carried out during 1991 and 1992. During each field experiments, the flow rate was kept constant by dams located upstream NPP. After each tritium release, water was sampled downstream at periodic intervals over several hours and tritium was measured with a low-background liquid scintillation counter. Velocity and dispersion coefficient were determined in river waters for several river discharges using an analytical, a box-type and a numerical approach to solve the one-dimensional advection-diffusion equation. The set of calibrated parameters was used to predict the displacement and the dispersion of soluble pollutants in river waters. Velocity was determined as a function of river discharge and river slope, and dispersion coefficient was determined as a function of distance. Finally, sensitivity of the model predictions was studied and uncertainties of the fitted parameters were estimated.

Keywords: River; water pollution; numerical methods; longitudinal dispersion coefficient; advection-diffusion equation.

INTRODUCTION

The hydrosphere represents an important pathway through which pollutants can be dispersed into the environment, become incorporated into the food chain, and hence to man (Eisenbud and Gesell, 1997). Regarding water quality control in rivers, both continuous pollution and accidental spills are the greatest ecological and economic potential dangers for rivers. In both cases, it is convenient to develop simple transport models in order to predict, with reasonable precision, concentration distributions and travel times of pollutants in rivers. The basic equation that describes the dispersion of pollutants in rivers is the one-dimensional advection-diffusion equation, which describes the dispersion as a function of mean stream velocity and a longitudinal dispersion coefficient (Leibundgut *et al.*, 1992). The one-dimensional advection-diffusion equation can be expressed as (Rutherford, 1994):

$$\frac{\partial c(x,t)}{\partial t} = D\frac{\partial^2 c(x,t)}{\partial x^2} - v\frac{\partial c(x,t)}{\partial x} \tag{1}$$

where $c(x,t)$ is the concentration of the substance or the solute, D is the dispersion coefficient, if assumed to be independent from x, and v is the mean velocity.

The mixing process of continuous release can be divided into three zones (Yotsukura and Sayre, 1976):

1. Initial mixing zone: the tracer is discharged into the river with an initial momentum and is not fully mixed. This zone extends from the source to a section where the distribution of the tracer concentration becomes uniform over depth, but not horizontally, and may cover a distance up to about one hundred times the river channel depth. In this first stage, three-dimensional equations are needed to study the dispersion.
2. Full mixing zone: the tracer has lost its initial momentum. This stage extends from the end of the initial mixing zone to a section where the tracer is mixed over the full

cross-section of the water body, that is vertically and horizontally, and may cover from 3 to 10 km in large rivers. The distance from the source to the point in which mixing is homogeneous and complete is known as the mixing length. To model this stage two-dimensional equations may suffice.

3. Far field dispersion zone: this stage extends from the end of the full mixing zone to a long distance, where the tracer concentration may become undetectable. One-dimensional equations are used to model this zone. Apart from convective transport, the predominant effect in this stage is longitudinal dispersion, that is, tracer cloud stretching in the velocity direction. This is predominant for instantaneous releases, but may also be observed in non-continuous releases such as those described in this work.

One of the important assumptions of the tracer dilution principle in the third zone is full mixing. In this case, and also for a continuous release under stationary hydraulic conditions, if $q << Q$, the tracer activity in the river (C_o) can be calculated as

$$C_o = \frac{C_t}{Q} q \tag{2}$$

where C_t is the mean concentration of tracer release, q is the flow rate of the tracer discharge and Q is the river discharge. This is valid for sampling points located at a distance from the source greater than the mixing length. A number of empirical formulae have been proposed to estimate the mixing length (Day, 1977; Guizerix and Florkowski, 1983; Rutherford, 1994). Nevertheless, the expressions should be used with caution as they have been empirically established for specific rivers in specific hydraulic conditions. In the case of the Ebro river, Asociación Nuclear Ascó observed that full heat mixing was always at 6.5 km from the release point for a range of hydraulic conditions (personal communication).

In this study, tritium routinely released as low-activity liquid radioactive waste by the Ascó nuclear power plant (Tarragona, Spain), was used to predict the displacement and the dispersion of soluble pollutants in the Ebro river in its lower course. We studied far-field tracer dispersion using the one-dimensional advection-diffusion equation with constant v and D. Predictive codes used the observed functional dependence of these two parameters with distance.

EXPERIMENTAL

Study area

The Ebro river is located in the Northeast of Spain and discharges into the Mediterranean sea after flowing for more than 900 km. The Ascó nuclear power plant is located in the final section of the river and comprises two pressurized-water reactor (PWR) units: Ascó I and Ascó II (Fig. 1). During their normal operation, these two units generate low-activity radioactive liquid waste, including tritium, which is released into the river in a controlled way: most activity is released from storage tanks, although a continuous release also exists. This routine operation can be used to trace river waters downstream.

A number of small streams discharge very small water quantities to the Ebro river. The largest tributary in this zone, river Ciurana (Fig. 1), contributes with less than 1 Hm^3 per year, which is much less than 1% of the Ebro river flow. Therefore, the presence of this tributary does not modify water flux of the main course of the Ebro river. On the other hand, water flow in the lower course of the Ebro river is highly regulated by dams. In particular, Ribaroja and Flix dams (Fig. 1) are located upstream from Ascó nuclear power plant.

Sampling

In order to study the hydrological dispersion of conservative pollutants in the lower course of Ebro river waters, several non-instantaneous tritium tank releases from Ascó nuclear power plant (Tarragona, Spain) were followed at different locations during 1991 and 1992, in coordination with the Ascó NPP (Pujol and Sanchez-Cabeza, 1999; Sanchez-Cabeza and Pujol, 1999). In 1991, seven different tank releases were followed at one location each time. In 1992, one tank release was followed at nine different locations during 19-20 May. During the field experiments, Ribaroja and Flix dams, upstream from Ascó kept the flow rate constant. The characteristics of each release are shown in Table 1.

Water was sampled from the river every 15 minutes during a total sampling period which ranged from 4 to 15 hours, depending on the distance from the nuclear power plant and the river flow. Special attention was given to the collection and preservation of samples (APHA-AWWA-WEF, 1992). Samples were collected in 125 ml polyethylene bottles, which had been carefully washed in the laboratory. Water was collected above the riverbed, sufficiently far from the river banks, natural or artificial obstacles, and avoiding stagnant or turbid water zones. Before the sample was collected, containers were rinsed three times with flowing river water. Simultaneous sampling from different points in the same cross-section at each sampling site was not carried out because it was assumed that the tracer was fully mixed in the river cross-section after the mixing length. Finally, samples were taken to the laboratory for analysis.

Analysis

As tritium is a soft beta emitter (5.72 keV mean energy), liquid scintillation is the most appropriate technique for its measurement. In this work, the low-background liquid

scintillation spectrometer Quantulus 1220 was used to determine tritium in river water samples (Pujol, 1996).

The analytical method used to determine tritium in river water samples was, briefly, the following: (*i*) samples were filtered through slow depth filters (such as Whatman 542), (*ii*) 8 ml of the filtrate was mixed and vigorously shaken during one minute with 12 ml of the scintillation cocktail OptiPhase Hisafe 3 (Wallac) in polyethylene vials (Wallac), (*iii*) three background samples and three tritium standards were simultaneously prepared, (*iv*) samples, backgrounds and tritium standards were stored in the liquid scintillation spectrometer during at least one day so that the chemiluminescence spectrum, which interferes with tritium measurements, had sufficiently decreased, and (*v*) samples, backgrounds and tritium standards were counted using Quantulus 1220 (Wallac). For a counting time of only 360 min, the detection limit (Currie, 1968) was 2.6 Bq litre^{-1} and the analytical uncertainties ranged from 5% to 30% (Pujol, 1996).

ALGORITHMS

Soluble pollutant dispersion in surface waters was modelled using analytical, box-type and numerical schemes (IAEA, 1985). In this work, eqn. 1 was solved for each type of approach.

The three approaches were based on the one-dimensional advection-diffusion equation with constant coefficients (both v and D do not depend on x). This initial assumption was made because water flux was kept constant during field experiments and the contribution to the water flux from tributaries was negligible. This first approximation provided a set of calibrated parameters needed to develop a simple predictive model.

Analytical approach

In our case, the boundary conditions required to solve the one-dimensional advection-diffusion equation were the following:

- The tritium pulsed release was described as a step function:

$$c(x,0) = C_i \tag{3}$$

$$c(0,t) = \begin{cases} C_0 & 0 < t \le t_0 \\ 0 & t > t_o \end{cases} \tag{4}$$

- To avoid any effect of the downstream boundary on results, a semi-infinite flow line was assumed (Kopman and Voss, 1987):

$$\frac{\partial c}{\partial x}(\infty,t) = 0 \tag{5}$$

Then, the analytical solution to the one-dimensional advection-diffusion equation was the following (Van Genuchten and Alves, 1982):

$$c(x,t) = \begin{cases} C_i + (C_0 - C_i)A(x,t) & 0 < t \le t_0 \\ C_i + (C_0 - C_i)A(x,t) - C_0 A(x,t-t_0) & t > t_0 \end{cases} \tag{6}$$

where

$$A(x,t) = \frac{1}{2}\operatorname{erfc}\left[\frac{x - vt}{2(Dt)^{1/2}}\right] + \frac{1}{2}\mathrm{e}^{-\frac{vx}{D}}\operatorname{erfc}\left[\frac{x + vt}{2(Dt)^{1/2}}\right] \tag{7}$$

and where erfc (x) is the complementary error function, and v and D are constant.

Box-type approach

The time evolution of the number of atoms of a given radionuclide in a compartment *i* is given by (Abril and García León, 1992):

$$\frac{\mathrm{d}}{\mathrm{d}t}N_\mathrm{i} = -k_{\mathrm{i},1}N_\mathrm{i} + k_{\mathrm{i}+1,2}N_{\mathrm{i}+1} + k_{\mathrm{i}-1,1}N_{\mathrm{i}-1} - k_{\mathrm{i},2}N_\mathrm{i} + Q_\mathrm{i}(t) - \lambda N_\mathrm{i} \tag{8}$$

where $Q_\mathrm{i}(t)$ includes all the radionuclide sources in the system and λ is the tritium radioactive decay constant. In our case, the radioactive decay term, λN_i, is negligible due to the rapidity of the phenomenon compared to the tritium half-life ($T_{1/2}$ = 12.43

years). The transfer coefficients between two adjacent compartments are given by the expressions:

$$k_{i,1} = \frac{v_i S_i}{V_i} + \frac{k_b S_i}{\Delta x_i V_i} \tag{9}$$

$$k_{i,2} = \frac{k_b S_i}{\Delta x_i V_i} \tag{10}$$

where $k_{i,1}$ is the transfer coefficient from compartment i to compartment i+1, $k_{i,2}$ is the transfer coefficient from compartment i to compartment i-1, k_b is a dispersion coefficient, V_i is the volume, S_i is the cross section and Δx_i is the length, all of them referred to compartment i. The first term on the right hand of expression 9 refers to convection and the second to dispersion. In expression 10 only dispersion is considered since there is no flow upstream (Abril and García León, 1992).

The water volume exchanged by a compartment i during Δt must be smaller than the volume V_i of the compartment. Mathematically, this can be expressed as $\Delta t << 1/k_{max}$, where k_{max} is the maximum coefficient in the whole system. On the other hand, the hypothesis of instantaneous and homogeneous mixing of a radionuclide input in a compartment produces numerical dispersion during calculation. This effect is equivalent to adding k_b' to the dispersion coefficient k_b according to the expression (Prandle, 1984)

$$k_b' = \frac{1}{2}(v\Delta x - v^2 \Delta t) \tag{11}$$

Then, the longitudinal dispersion coefficient of eqn 1 can be expressed as

$$D = k_b + k_b' \tag{12}$$

It can be shown that numerical dispersion presents a minimal value given by the following relationship (Pujol, 1996):

$$k'_{b\,min} = \frac{1}{2}\left(\frac{1}{v\,\Delta x} + \frac{1}{k_b}\right)^{-1} \tag{13}$$

There are two conditions for which the determination of the dispersion coefficient (D) is not possible: i) if $k_b' < k_b'_{min}$, the solution is unstable, or ii) if $k_b' > D$, the value of k_b is indefinite.

The optimization of the spatial and temporal resolution led us to choose Δx = 100 m and Δt = 15 s, or Δx = 250 m and Δt = 60 s, depending on the distance (Table 3). For these steps, the solution of eqn 1 was stable.

In principle, the analytical and the box-type approaches were not equivalent from a mathematical point of view because the last was based on a set of equations that described the diffusion and the transport by using values of D and v that were functions of the position. Nevertheless, to solve eqn 1, constant volume, cross section and length were assumed for all the boxes, and then transfer coefficients were also kept constant.

Numerical approach

The solution of the one-dimensional advection-diffusion equation using an explicit finite differences method can be obtained from the following expression:

$$c_{x,t+\Delta t} = \frac{D\Delta t}{(\Delta x)^2} c_{x+\Delta x,t} + \left(1 - 2\frac{D\Delta t}{(\Delta x)^2} - \frac{v\Delta t}{\Delta x}\right) c_{x,t} + \left(\frac{D\Delta t}{(\Delta x)^2} + \frac{\Delta t v}{\Delta x}\right) c_{x-\Delta x,t} \quad (14)$$

where $c_{x,t+\Delta t}$ is the mean cross-sectional concentration as a function of time for a distance x from the emission point, and v and D are constant. The eqn 14 is stable if (Noye, 1987):

$$\frac{D\Delta t}{\Delta x^2} \leq \frac{\left(1 - \frac{\Delta t v}{\Delta x}\right)}{2} \quad (15)$$

The optimization of the spatial and temporal resolution led us to choose Δx = 100 m and Δt = 15 s, respectively, for which the solution was stable.

Longitudinal dispersion coefficient and mean velocity

Several computer codes were written to generate solutions of the advection-diffusion equation for each approach and for the two parameter values (longitudinal dispersion coefficient and mean velocity) at all the considered locations. For each solution and measured tritium concentration time-distribution, chi-square (χ^2) was computed using the following expression:

$$\chi^2 = \sum_{i=1}^{k} \frac{(F_i - \phi_i)^2}{\phi_i} \tag{16}$$

where F_i are the experimental data and ϕ_i are the theoretical values generated from each approach. The fitted solution was obtained by minimisation of χ^2 by varying both D and v (Fig. 2), and was considered statistically acceptable if $\chi^2 \leq \chi^2_\varepsilon$, where χ^2_ε is the decision limit with an ε significance level, usually chosen as $\varepsilon = 0.05$. D and v values for which χ^2 was minimum were called optimized longitudinal dispersion coefficient (D_o) and optimized velocity (v_o). As an example, the observed and fitted (box-type approach) tritium concentration distribution in Mora de Ebro town is represented (Fig. 3).

Fitted parameter uncertainties

The method used to estimate parameter uncertainties is briefly explained below (Myers, 1986; Rawlings, 1988). Let us consider a set of experimental data: x_i (independent variable), y_i (dependent variable) and $i = 1, 2, ..., n$ (experimental observations). These data were fitted to a function such that $y_i = f(x_i, \alpha, \beta)$, where α and β were two parameters estimated through the chi-square test. Then, the uncertainties associated to each parameter (σ_α and σ_β) were determined by computing the square root of the diagonal elements of the matrix $s^2(W'W)^{-1}$, where:

$$s^2 = \frac{\sum (y_i - \hat{y}_i)^2}{n-2} \tag{17}$$

s is the standard deviation and $\hat{y}_i$ the dependent variable estimator. The matrix $(W'W)^{-1}$ is the covariance matrix, and W' is the transposed matrix of W, which elements are

$$w_{ji} = \left(\frac{\partial f(x_i, \theta_j)}{\partial \theta_j} \right) \tag{18}$$

where θ_j are the parameter estimate ($\theta_1 = \alpha$, $\theta_2 = \beta$). The derivatives were evaluated for the fitted parameters.

Discussion

The optimized longitudinal dispersion coefficient and mean velocity for each field experiment and solution approach are shown in Table 2. The optimized longitudinal dispersion coefficient showed great variability, as it ranged from 41 ± 30 $m^2\ s^{-1}$ to 392 ± 45 $m^2\ s^{-1}$. Although the fitted parameters were similar for all approaches, values obtained with the numerical approach were, in general, lower than those obtained with the analytical and box-type approaches. This phenomenon has also been observed by other authors and is due to numerical dispersion (Noye, 1987). Although other methods, such as the Lax-Wendroff method, would avoid this problem, this was not considered essential for the purpose of this work.

The optimized mean water velocity showed limited variation, as it ranged from 0.558 ± 0.011 m s^{-1} to 1.278 ± 0.019 m s^{-1} and the values obtained from the three approaches at each location were statistically indistinguishable.

In most cases, model fittings were satisfactory as all showed $\chi^2 < \chi^2_{0.05}$. In some locations, the larger χ^2 values observed were due, mainly, to the long tails of the tritium pulses (Fig. 3). Several authors have successfully proposed a dead zone model in which a term is added to the one-dimensional diffusion equation to allow for temporary

entrapment of portions of the tracer in the dead zones (Nordin and Troutman, 1980; Yu and Wenzhi, 1989), although this was not the objective of the present work.

PREDICTIVE CODES

Predictive computer codes, written in FORTRAN 77, were calibrated by optimising velocity and longitudinal dispersion coefficient. The three approaches were used to predict the dispersion of tritium in the Ebro river waters downstream from the Ascó nuclear power plant using diverse algorithms.

The dependence of optimized v and D on the distance was studied (Table 2). Through these results, a relationship between velocity and distance (see Velocity calibration), and between longitudinal dispersion coefficient and distance (see Longitudinal dispersion calibration) was determined. Therefore, predictive computer codes considered the dependence both v and D on x. The computer codes of the analytical, box-type and numerical approach were named PREANA, PREBOX and PRENUM, respectively. Initial river conditions (river discharge, duration of the release, total tritium activity released and distance between Ascó nuclear power plant and the location where prediction was done) were needed to run the codes. Results were presented as a file with tritium concentration in function of time for the selected distance.

A summary of the parameters used in the predictive computer programs for all the approaches are shown in Table 3. For each approach, both the uncertainty of the velocity and the maximum travel time pulse prediction were determined using the covariance matrix. The uncertainty (σ) of a prediction was determined through (Myers, 1986; Rawlings, 1988)

$$\sigma = s\sqrt{1+\mathbf{x}_i'\left(W'W\right)^{-1}\mathbf{x}_i} \tag{19}$$

where s and W were defined in eqn 17 and 18, respectively, x_i is the row vector corresponding to the i row from the W matrix, x_i' is the transpose of x_i. Notice that x_i is evaluated at the point of interest.

Velocity calibration

Velocity can be determined in rivers through the Manning equation (Chow *et al*., 1988; Gordon *et al*., 1992):

$$v = \frac{R^{2/3} S^{1/2}}{\eta} \tag{20}$$

where R is the hydraulic radius (defined as $R = A/P$, where A is the cross-sectional area of the flow and P is the wetted perimeter), S is the slope of the river and η is the Manning roughness coefficient. The application of this relationship in the Ebro river was not possible because of the scarce knowledge of the river geometry. In these cases, river discharge (Q) can be related to velocity (or other dependent variable such as width, mean depth, slope and so on) through a power relationship (Knighton, 1984; Morisawa, 1985):

$$v = r\, Q^m \tag{21}$$

where r and m are coefficients to be determined. However, we proposed the following relationship for the predictive approaches because it provided a better fitting (Fig. 4) (Pujol, 1996):

$$v = a\left(1 - e^{-\frac{(Q+b)}{c}}\right) \tag{22}$$

where a, b and c are coefficients to be determined.

On the other hand, it was observed that velocity depended on river slope and this was different for each sampling location. Then, the slope at each location was estimated using the following relationship (Knighton, 1984):

$$S = w\,L^{z} \tag{23}$$

where L is the distance from the release point, and w and z are coefficients to be determined. Therefore, eqn 20 and 23 led us to expression:

$$v = w'\,L^{z'} \tag{24}$$

where w' and z' are coefficients to be determined. Then, a relationship between velocity and distance was estimated through experimental data (May 19-20th, 1992) in which river discharge was constant for all the sampling locations. This relationship led us to a function named *velocity decrease factor* (F_d):

$$F_d = w''L^{z''} \tag{25}$$

where w'' and z'' are coefficients to be determined. Then, velocity was computed in each location using the resulting relationship:

$$v = w''L^{z''}a\left(1 - e^{-\frac{(Q+b)}{c}}\right) \tag{26}$$

Longitudinal dispersion calibration

The longitudinal dispersion coefficient in rivers depends on several factors, such as river discharge, mean depth, shear velocity, channel width and dead zones. In consequence, the most accurate method to determine the longitudinal dispersion coefficient in rivers is experimentally using a tracer. In eqn 1, D is assumed to be constant, which reduces complexity of the solutions and, in this study, permitted the comparison of the various approaches to solve the proposed problem. However, this was not the case, as the coefficient is largely dependent on river flow and morphology. A more complete study on the hydrodynamics of the river should consider its variability with these, although this was not the objective of the present work.

The variation of the longitudinal dispersion coefficient with distance from the release point showed three distinct zones (Sanchez-Cabeza and Pujol, 1999):

1. From Ascó to García (0-11.0 km from the release point): the longitudinal dispersion coefficient at Pas de l'Ase and García (from 5 ± 31 m^2 s^{-1} to 106 ± 17 m^2 s^{-1}) was relatively low. As a consequence, the tritium peak concentrations were relatively sharp and maximum concentration decreased moderately between the two locations.
2. From García to Miravet (11.0-28.0 km): larger longitudinal dispersion coefficients (from 171 ± 34 m^2 s^{-1} to 392 ± 45 m^2 s^{-1}) caused important diffusion in this section. As a consequence, the tritium concentration peak flattened and broadened considerably at Mora de Ebro in relation to García, in the previous zone. Furthermore, both peaks at Mora de Ebro and Miravet showed long tails which indicated the presence of dead zones in this section. This is due to the increase of width channel and the decrease of river depth, including island deposition.
3. From Miravet to Tortosa (28.0-63.5 km): in this zone the maximum tritium concentration decreased only slightly and the peak shape was more symmetrical and almost unchanged from Benifallet. This was in agreement with lower longitudinal dispersion coefficients (from 149 ± 18 m^2 s^{-1} to 52 ± 2 m^2 s^{-1}) which caused little effect on the tracer distribution shape. Downstream Xerta, tracer transport became more complex because a channel diverts some water at this location and downstream Tortosa estuarine effects start to become apparent.

For the elaboration of predictive computer codes, longitudinal dispersion coefficient was assumed to be constant from Ascó to García (zone 1) and from Mora de Ebro to Miravet (zone 2). On the other hand, a power dependence with distance was considered from Benifallet to Tortosa (zone 3). In the sections between zone 1 and 2, and zone 2 and 3, a linear relationship was assumed.

SENSITIVITY ANALYSIS

The sensitivity of model predictions to changes in the parameter values is known as

sensitivity analysis of the model. This analysis reveals not only the robustness of the model but also provides an insight into the importance of the various mechanisms involved. Often, parameters included in models are not known precisely. In this case, results produced by the model will be acceptable if predictions are not altered significantly when parameters are varied within their respective uncertainty margins (Prandle, 1984; IAEA, 1986).

In this work, sensitivity analysis was carried out varying the predicted dispersion coefficient (D_p) and the predicted velocity (v_p) within their uncertainty margins for two locations: one next to the release point (Pas de l'Ase, May 6th, 1991) and the other far from the release point (Tortosa, May 20th, 1992). Both localities were also used to determine the effect of the distance on the analyzed parameters.

Dispersion coefficient variation

In Pas de l'Ase, it was observed that the variation of the dispersion coefficient within its respective uncertainty margins did not significantly modify model predictions (Fig. 5a). For long distances, that is, in Tortosa (Fig 5b), the three approaches did not show significant differences.

Velocity variation

In Pas de l'Ase, it was observed that the variation of the velocity within its respective uncertainty margins did not significantly modify model predictions (Fig. 5c). In Tortosa, it was observed that model predictions were systematically shifted (Fig. 5d). This was because the uncertainty was greater far away from the release point (Table 4).

MODEL VALIDATION

Model validation was carried out using sampling data. Computer programs were used to determine tritium concentration in Pas de l'Ase on May 6th 1991 (Fig. 6a), in Miravet

on December 16th 1991 (Fig. 6b), and in Tortosa on May 20th 1992 (Fig 6c). These locations were selected because they presented a different behaviour in dispersion coefficient. Table 4 shows that velocity, maximum travel time, maximum tritium concentration and dispersion coefficient predictions were similar using numerical, box-type and analytical approaches for the selected locations.

Predictions using the analytical approach were rapid. On the other hand, for long distances, the box-type and numerical approaches were slow because of the numerous operations needed to solve the computer algorithm. For instance, in Tortosa, the box-type approach needed about two minutes and the numerical approach needed around half an hour using a DX2/486 (66 MHz) personal computer. This difference was because, for long distances, the spatial and temporal grids were greater in the box-type than in the numerical approach. Box-type and numerical approaches were more expensive in computing time than the analytical approach.

The analytical approach was useful because predictions were good with a small computing time. However, the addition of more terms to the one-dimensional advection-diffusion equation in order to consider other physical phenomena or boundary conditions requires box-type or numerical approaches in order to solve the resulting differential equation.

CONCLUSIONS

The one-dimensional advection-diffusion equation was solved for the case of non-instantaneous tracer release. Longitudinal dispersion coefficient and velocity were determined using three different approaches: analytical, box-type and numerical. Approaches showed similar results, with greater similarity between box-type and analytical approaches. Box-type and numerical approaches were more expensive in terms of computing time.

For the river discharge studied, ranging from 178 to 915 $m^3\ s^{-1}$, longitudinal dispersion coefficient ranged from 5 ± 31 to 392 ± 45 $m^2\ s^{-1}$ and mean velocities ranged from 0.558 ± 0.011 to 1.278 ± 0.019 m s^{-1}.

The calibration of velocity and dispersion coefficient were necessary to elaborate computer codes to predict the dispersion. Velocity was determined as a function of river discharge and river slope, and dispersion coefficient was determined as a function of distance. The uncertainty of velocity, maximum travel time and dispersion coefficient prediction was determined for every approach using the covariance matrix. Sensitivity analysis in velocity and dispersion coefficient showed the robustness of the predictions.

The results of this work can be used to predict the movement and dispersion of a soluble pollutant in the Ebro river downstream the nuclear power plant and assist in the design of adequate surveillance programmes and emergency actions in the case of the accidental release of any soluble pollutant.

LIST OF SYMBOLS

Symbol	Unit	Definition
$A(x,t)$		Mathematical function.
A	m^2	Cross-sectional area.
$c(x,t)$	Bq $litre^{-1}$	Mean cross-sectional concentration of the substance or tracer.
$c_{x,t+\Delta t}$	Bq $litre^{-1}$	Mean cross-sectional concentration, as a function of time, for a distance x from the emission point (explicit numerical approach).
c_i^{exp}	Bq $litre^{-1}$	Experimental tritium concentration.
c_i^{the}	Bq $litre^{-1}$	Theoretical tritium concentration for one approach.
C_i	Bq $litre^{-1}$	Background concentration of the tracer.

C_0	Bq litre^{-1}	Initial mean cross-sectional concentration after total mixing.
C_t	Bq litre^{-1}	Mean concentration of tracer release.
D	m^2 s^{-1}	Longitudinal dispersion coefficient.
D_o	m^2 s^{-1}	Optimized longitudinal dispersion coefficient.
D_p	m^2 s^{-1}	Predicted longitudinal dispersion coefficient.
D_+	m^2 s^{-1}	Predicted longitudinal dispersion coefficient plus uncertainty.
D_-	m^2 s^{-1}	Predicted longitudinal dispersion coefficient minus uncertainty.
erfc(x)		Complementary error function.
F_i		Experimental data for chi–square fitting.
F_d		Decrease factor of the velocity.
L	m	Distance from the release point.
k_b	m^2 s^{-1}	Dispersion coefficient in the box–type approach.
k_b'	m^2 s^{-1}	Numerical dispersion coefficient in the box–type approach.
$k_{i,1}$	s^{-1}	Transfer coefficient from compartment i to compartment i+1.
$k_{i,2}$	s^{-1}	Transfer coefficient from compartment i to compartment i-1.
k_{max}	s^{-1}	Maximum transfer coefficient in the whole system.
n		Number of experimental observations.
N_i		Tracer particles in box i.
P	m	Wetted perimeter.
q	m^3 s^{-1}	Flow rate of the tracer discharge.
Q	m^3 s^{-1}	River discharge.
$Q_i(t)$	part. s^{-1}	Tracer sources.
R	m	Hydraulic radius.
s^2		Variance.
S		Slope of the river.

S_i	m^2	Cross section of compartment i.
t	s	Time.
t_0	s	Duration of the release.
Δt	s	Temporal resolution of the box–type and numerical approaches.
v	$m\ s^{-1}$	Mean flow velocity.
v_c	$m\ s^{-1}$	Calibrated velocity.
v_o	$m\ s^{-1}$	Optimized velocity.
v_p	$m\ s^{-1}$	Predicted velocity.
v_+	$m\ s^{-1}$	Predicted velocity plus uncertainty.
v_-	$m\ s^{-1}$	Predicted velocity minus uncertainty.
V_i	m^3	Volume of compartment i.
W		Derivative of a function in respect of the parameters estimate (matrix).
W'		Transpose of the matrix W.
$(W'W)^{-1}$		Covariance matrix.
x	m	Cartesian coordinate in the flow direction.
x_i		Independent variable.
Δx	m	Spatial resolution of the box–type and numerical approaches.
Δx_i	m	Length of the compartment i.
y_i		Dependent variable.
$\hat{y}_i$		Estimate value of the dependent variable.
α		Parameter estimated in an approach.
β		Parameter estimated in an approach.
ε		Statistical significance risk level.
η		Manning roughness coefficient.

χ^2	Chi-square.
χ^2_ε	Statistically significant χ^2 with a risk level ε.
λ	Decay constant.
ϕ_i	Theoretical data for chi–square fitting.
θ_j	General parameter estimated in an approach.
σ_α	Uncertainty in the α parameter.
σ_β	Uncertainty in the β parameter.

ACKNOWLEDGEMENTS

Financial support received from *Junta de Sanejament de la Generalitat de Catalunya* is gratefully acknowledged. Also, we wish to express our gratitude to Asociación Nuclear Ascó for its collaboration in this study and for supplying important information for its scientific development, and to Confederación Hidrográfica del Ebro, Embalse de Ribaroja and Embalse de Flix for their collaboration in maintaining constant flow rate during the sampling campaigns. Thanks are due to our colleagues in the Physics Department for their collaboration in sampling campaigns.

REFERENCES

Abril, J.M. and García León, M. (1992) A marine dispersion model for radionuclides and its calibration from non-radiological information. *Journal of Environmental Radioactivity* **16**, 127-146.

APHA-AWWA-WEF (1992*) Standard Methods for the Examination of Water and Wastewater*. American Public Health Association, Washington.

Chow, V.T., Maidment, D.R. and Mays, L.W. (1988) *Applied Hydrology*. McGraw-Hill Book Company, New York, 572 pp.

Currie, L.A. (1968) Limits for qualitative detection and quantitative determination. *Analytical Chemistry* **40**, 586-592.

Day, T.J. (1977) Observed mixing lengths in mountain streams, *Journal of Hydrology* **35**, 125-136.

Eisenbud, M. and Gesell, T. (1997) *Environmental Radioactivity*. Academic Press, San Diego, 656 pp.

Gordon, N.D., McMahon, T.A. and Finlayson, B.L. (1992) *Stream Hydrology*. John Wiley & Sons, Chichester, 526 pp.

Guizerix J. and Florkowski, T. (1983) Streamflow measurements. In *Guidebook on Nuclear Techniques in Hydrology*, pp. 65-79. IAEA, Vienna.

IAEA (1985) Hydrological dispersion of radioactive material in relation to nuclear power plant siting. Safety Series nº 50-SG-S6, International Atomic Energy Agency, Vienna, 116 pp.

IAEA (1986) An oceanographic model for the dispersion of wastes disposed of in the deep sea. Technical Reports Series nº 263, International Atomic Energy Agency, Vienna, 166 pp.

Knighton, D. (1984) *Fluvial Forms and Processes*. Edward Arnold, London, 218 pp.

Kopman, D.B. and Voss, C.I. (1987) Behaviour of sensitivities in the one-dimensional advection-dispersion equation: implications for parameter estimation and sampling design. *Water Resources Research* **23**, 253-272.

Leibundgut, Ch., Speidel, U., Wiesner, H. and van Mazijk, A. (1992) Investigation of flow and transport parameters in rivers. In *Tracer Hydrology*, ed. H. Hötzl & A. Werner, pp. 379-385. A.A. Balkema, Rotterdam.

Morisawa, M. (1985) *Rivers*. Longman Group Limited, New York, 222 pp.

Myers, R.H. (1986) *Classical and Modern Regression with Applications*. PWS

Publishers, Boston, Massachusetts, 359 pp.

Nordin, C.F. and Troutman, B.M. (1980) Longitudinal dispersion in rivers: the persistence of skewness in observed data. *Water Resources Research* **16**, 123-128.

Noye, J. (1987) Finite difference methods for solving one-dimensional transport equation. In *Numerical modelling: Applications to marine systems*, ed. J. Noye, pp. 231-256. Elsevier Science Publishers B.V., North-Holland.

Prandle, D. (1984) A modelling study of the mixing of ^{137}Cs in the seas of the european continental shelf. *Phil. Trans. Royal Society London*, **A310**, 407-436 .

Pujol, Ll. (1996) Radiactividad del Agua Superficial y los Sedimentos en la Cuenca del Ebro. Utilización del Tritio como Radiotrazador en el Tramo Catalán, Ph.D. thesis, Universitat Autònoma de Barcelona, Spain (in Spanish).

Pujol, Ll. and Sanchez-Cabeza, J.A. (1999) Determination of longitudinal dispersion coefficient and velocity of the Ebro river waters (Northeast Spain) using tritium as a radiotracer. *Journal of Environmental Radioactivity* **45**, 39-57.

Rawlings, J.O. (1988) *Applied Regression Analysis*. A Research Tool. Wadsworth, Inc., California, 553 pp.

Rutherford, J.C. (1994) *River Mixing*. John Willey and Sons, New York, 347 pp.

Sanchez-Cabeza, J.A. and Pujol, Ll. (1999) Study on the hydrodynamics of the Ebro river lower course using tritium as a radiotracer. *Water Research* (in press).

Van Genuchten, M.T. and Alves, W.J. (1982) *Analytical Solutions of the One-Dimensional Convective-Dispersive Solute transport Equation*. United States Department of Agriculture, Washington, 149 pp.

Yotsukura, N. and Sayre, W.W. (1976) Transverse mixing in natural channels. *Water Resources Research* **12**, 695-704.

Yu, Y.S. and Wenzhi, L. (1989) Longitudinal dispersion in rivers: a dead-zone model

solution. *Water Resources Bulletin* **25**, 319-325.

Table 1. Characteristics of the tritium releases monitored in Ebro river waters downstream Ascó Nuclear Power Plant during 1991 and 1992

Date	Sampling location	Distance (km)	Release duration† (min)	Tritium activity† (GBq)	River discharge¶ (m^3 s^{-1})	Mixing activity (Bq $litre^{-1}$)
May 6, 1991	Pas de l'Ase	6.5	110	136.2	915	22.6
July 15, 1991	García	11.0	126	19.2	178	14.3
Aug. 5, 1991	Mora de Ebro	16.0	67	47.4	211	56.0
Dec. 5, 1991	Mora de Ebro	16.0	60	279.8	626	124
Dec. 9, 1991	Ascó	0.5	42	222.1	390	226
Dec. 13, 1991	García	11.0	49	10.3	359	9.7
Dec. 16, 1991	Miravet	28.0	72	329.2	348	219
May 19, 1992	(‡)	(‡)	105	76.5	220	55.2

†Ascó Nuclear Power Plant, personal communication.

¶ Flix dam, personal communication.

(‡) Locations: Ascó (0.5 km), Pas de l'Ase (6.5 km), García (11.0 km), Mora de Ebro (16.0 km), Miravet (28.0 km), Benifallet (39.0 km), Xerta (47.5 km), Tortosa (63.5 km) and Amposta (78.0 km).

Table 2. Summary of the optimised parameters determined with the different approaches

Location	Distance (km)	Approach	v (m s^{-1})	D (m^2 s^{-1})	χ^2	$\chi^2_{0.05}$
Pas de l'Ase	6.5	Analytical	1.247 ± 0.017	101 ± 26	0.8	14.1
(May 6, 1991)		Box-type	1.278 ± 0.019	104 ± 27	0.9	14.1
		Numerical	1.247 ± 0.017	50 ± 27	0.9	14.1
García	11.0	Analytical	0.563 ± 0.011	48 ± 18	9.8	21.0
(July 15, 1991)		Box-type	0.567 ± 0.011	48 ± 18	9.7	21.0
		Numerical	0.558 ± 0.011	22 ± 18	9.7	21.0
Mora de Ebro	16.0	Analytical	1.119 ± 0.015	218 ± 34	35.2	21.0
(Dec. 5, 1991)		Box-type	1.146 ± 0.015	222 ± 36	36.3	21.0
		Numerical	1.119 ± 0.015	171 ± 34	35.3	21.0
García	11.0	Analytical	0.847 ± 0.027	41 ± 30	5.0	7.8
(Dec. 13, 1991)		Box-type	0.852 ± 0.028	42 ± 31	4.9	7.8
		Numerical	0.844 ± 0.028	5 ± 31	4.9	7.8
Miravet	28.0	Analytical	0.858 ± 0.011	379 ± 45	88.6	38.9
(Dec. 16, 1991)		Box-type	0.884 ± 0.011	392 ± 45	87.6	38.9
		Numerical	0.855 ± 0.010	290 ± 41	78.1	38.9
Pas de l'Ase	6.5	Analytical	0.689 ± 0.013	67 ± 20	12.3	18.3
(May 19, 1992)		Box-type	0.710 ± 0.014	70 ± 21	12.2	18.3
		Numerical	0.689 ± 0.013	36 ± 20	12.2	18.3
García	11.0	Analytical	0.645 ± 0.009	104 ± 17	15.0	23.7
(May 19, 1992)		Box-type	0.663 ± 0.009	106 ± 17	15.2	23.7
		Numerical	0.645 ± 0.009	75 ± 17	14.8	23.7
Mora de Ebro	16.0	Analytical	0.580 ± 0.011	256 ± 35	21.0	30.1
(May 19, 1992)		Box-type	0.611 ± 0.011	264 ± 35	20.5	30.1
		Numerical	0.579 ± 0.011	230 ± 35	20.7	30.1
Miravet	28.0	Analytical	0.664 ± 0.009	257 ± 37	32.9	38.9
(May 19-20, 1992)		Box-type	0.682 ± 0.009	261 ± 36	31.9	38.9
		Numerical	0.664 ± 0.009	228 ± 37	32.4	38.9
Benifallet	39.0	Analytical	0.652 ± 0.005	147 ± 18	25.4	38.9
(May 19-20, 1992)		Box-type	0.656 ± 0.005	149 ± 18	23.7	38.9
		Numerical	0.648 ± 0.005	118 ± 18	24.9	38.9
Xerta	47.5	Analytical	0.577 ± 0.002	90 ± 6	6.9	33.9
(May 19-20, 1992)		Box-type	0.579 ± 0.002	90 ± 6	6.1	33.9
		Numerical	0.575 ± 0.002	64 ± 6	6.7	33.9
Tortosa	63.5	Analytical	0.585 ± 0.001	79 ± 2	0.6	23.7
(May 20, 1992)		Box-type	0.587 ± 0.001	79 ± 2	0.6	23.7
		Numerical	0.584 ± 0.001	52 ± 2	0.6	23.7

Uncertainties correspond to ± 1σ.

Table 3. Summary of the parameters in the predictive computer codes

Code computer	PREANA	PREBOX	PRENUM
Approach	Analytical	Box-type	Numerical
Spatial and temporal resolution		100 m, 15 s (Pas de l'Ase and García) 250 m, 60 s. (from Mora de Ebro)	100 m 15 s
F_d	$1.129\ L^{-0.0649}$	$1.148\ L^{-0.07388}$	$1.116\ L^{-0.0588}$
Velocity	$F_d\ (1.314 \pm 0.067)\left(1 - e^{-\frac{Q-(13\pm35)}{284\pm65}}\right)$	$F_d\ (1.343 \pm 0.069)\left(1 - e^{-\frac{Q-(16\pm36)}{275\pm65}}\right)$	$F_d\ (1.321 \pm 0.067)\left(1 - e^{-\frac{Q-(12\pm34)}{289\pm65}}\right)$
Dispersion coefficient		$D = k_b + k_b'$	
6.5 km ≤ L ≤ 11.0 km	72 ± 31	74 ± 31	46 ± 22
11.0 km < L < 16.0 km	-306 + 34.4 *L*	-390 + 42.2 *L*	-359 + 36.8 *L*
16.0 km ≤ L ≤ 28.0 km	244 ± 30	285 ± 76	230 ± 52
28.0 km < L < 39.0 km	531 - 10.3 *L*	662 - 13.5 *L*	553 - 11.5 *L*
39.0 km ≤ L ≤ 63.5 km	$(72 \pm 35)\ 10^2\ \ L^{-(1.09 \pm 0.14)}$	$(151 \pm 65)\ 10^2\ L^{-(1.28 \pm 0.13)}$	$(18 \pm 10)\ 10^3\ \ L^{-(1.41 \pm 0.17)}$

Uncertainties correspond to ± 1σ.

Table 4. Experimental and predictive data for some parameters (v: velocity; T_{max}: maximum travel time; C_o: maximum tritium concentration; D: dispersion coefficient;CT: computing time)

	v (m s^{-1})	T_{max} (min)	C_o (Bq $litre^{-1}$)	D (m^2 s^{-1})	χ^2	$\chi^2_{0.05}$	CT (s)†
Pas de l'Ase (May 6, 1991)							
Experimental	1.247 ± 0.017	142 ± 1	22.6	101 ± 26	0.8	14.1	
PRENUM	1.26 ± 0.05	141 ± 4	22.6	46 ± 22	1.0	12.6	18
PREBOX	1.29 ± 0.06	139 ± 4	22.5	74 ± 31	2.1	14.1	18
PREANA	1.26 ± 0.05	141 ± 4	22.5	72 ± 31	1.4	14.1	1
Miravet (Dec. 16, 1991)							
Experimental	0.858 ± 0.011	579 ± 7	63.9	379 ± 45	88.5	38.9	
PRENUM	0.83 ± 0.04	597 ± 28	74.0	230 ± 52	123.0	37.7	221
PREBOX	0.84 ± 0.05	589 ± 30	72.2	285 ± 76	139.7	35.2	24
PREANA	0.83 ± 0.04	599 ± 29	76.1	244 ± 30	156.1	35.2	1
Tortosa (May 20, 1992)							
Experimental	0.585 ± 0.001	1862 ± 3	18.9	79 ± 2	0.6	23.7	
PRENUM	0.59 ± 0.04	(184 ± 11)·10^1	19.4	52 ± 17	5.0	23.7	1567
PREBOX	0.60 ± 0.04	(184 ± 12)·10^1	20.2	73 ± 19	4.3	23.7	166
PREANA	0.60 ± 0.04	(185 ± 11)·10^1	19.3	77 ± 16	1.0	23.7	1

Uncertainties correspond to ± 1σ.

† For a DX2/486 (66 MHz) personal computer.

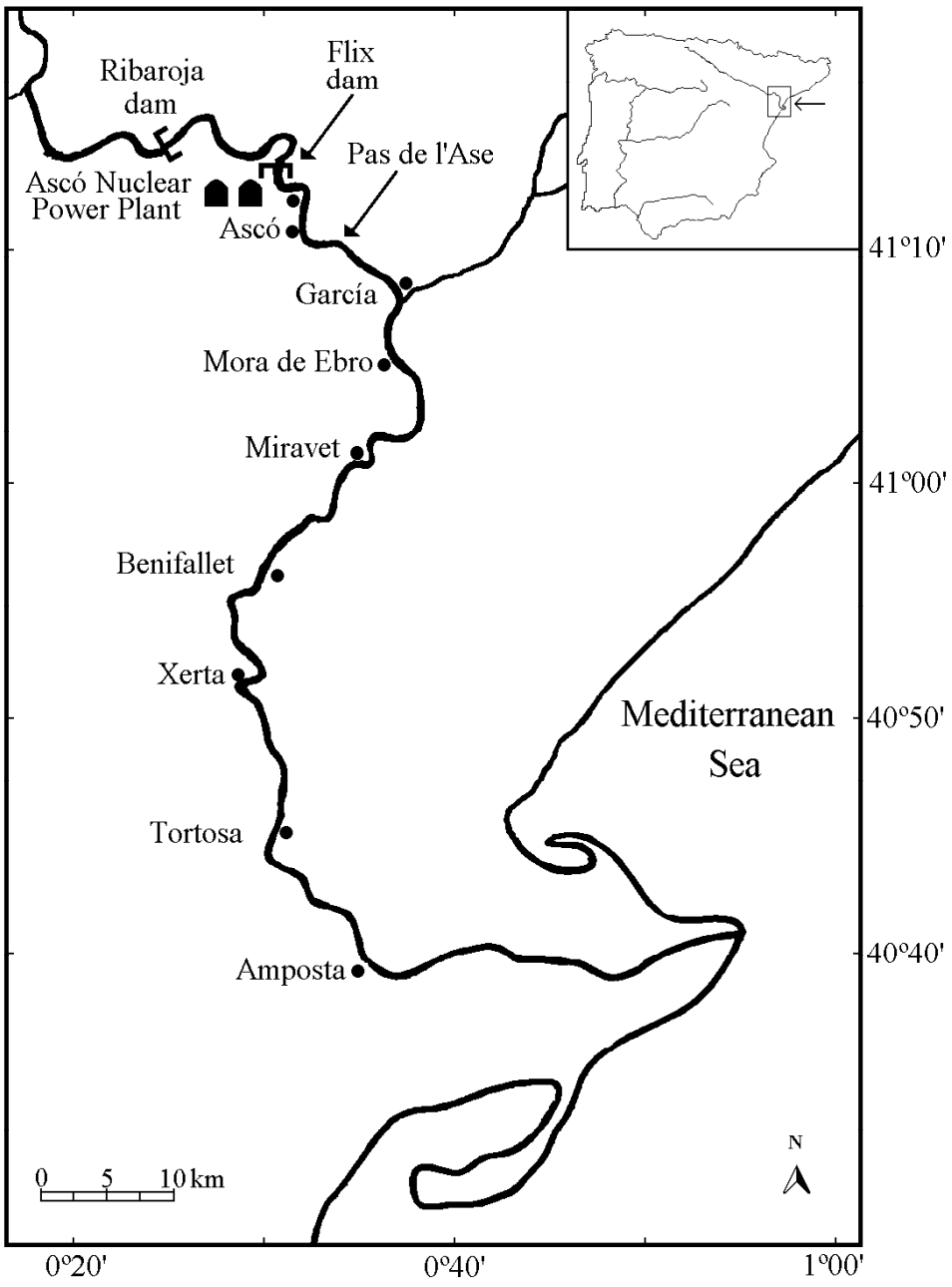

Fig. 1. Map of the studied Ebro river section showing sampling locations.

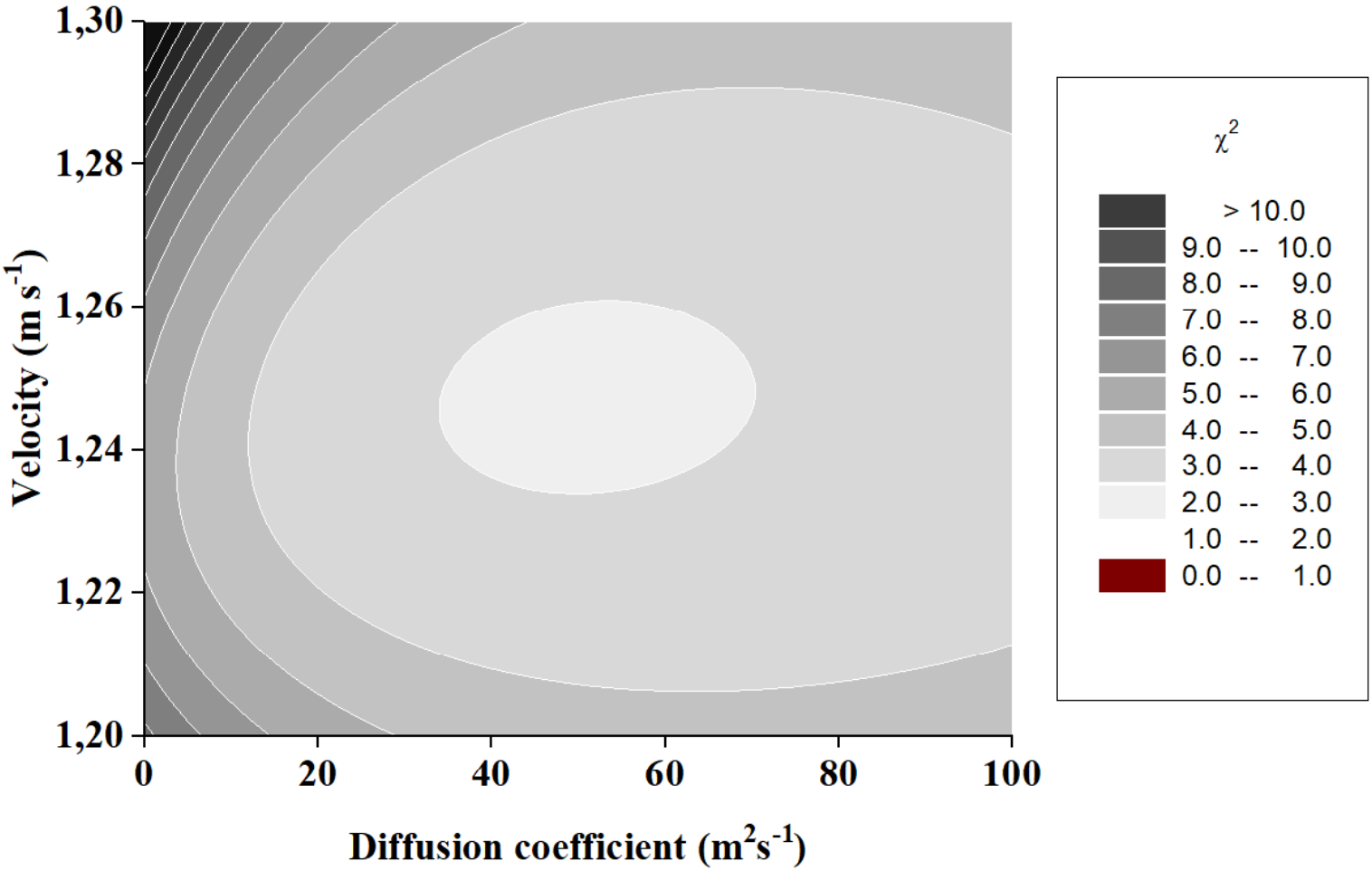

Fig. 2. Determination of the optimum velocity and dispersion coefficient parameters using the numerical approach for Pas de l'Ase on May 6, 1991.

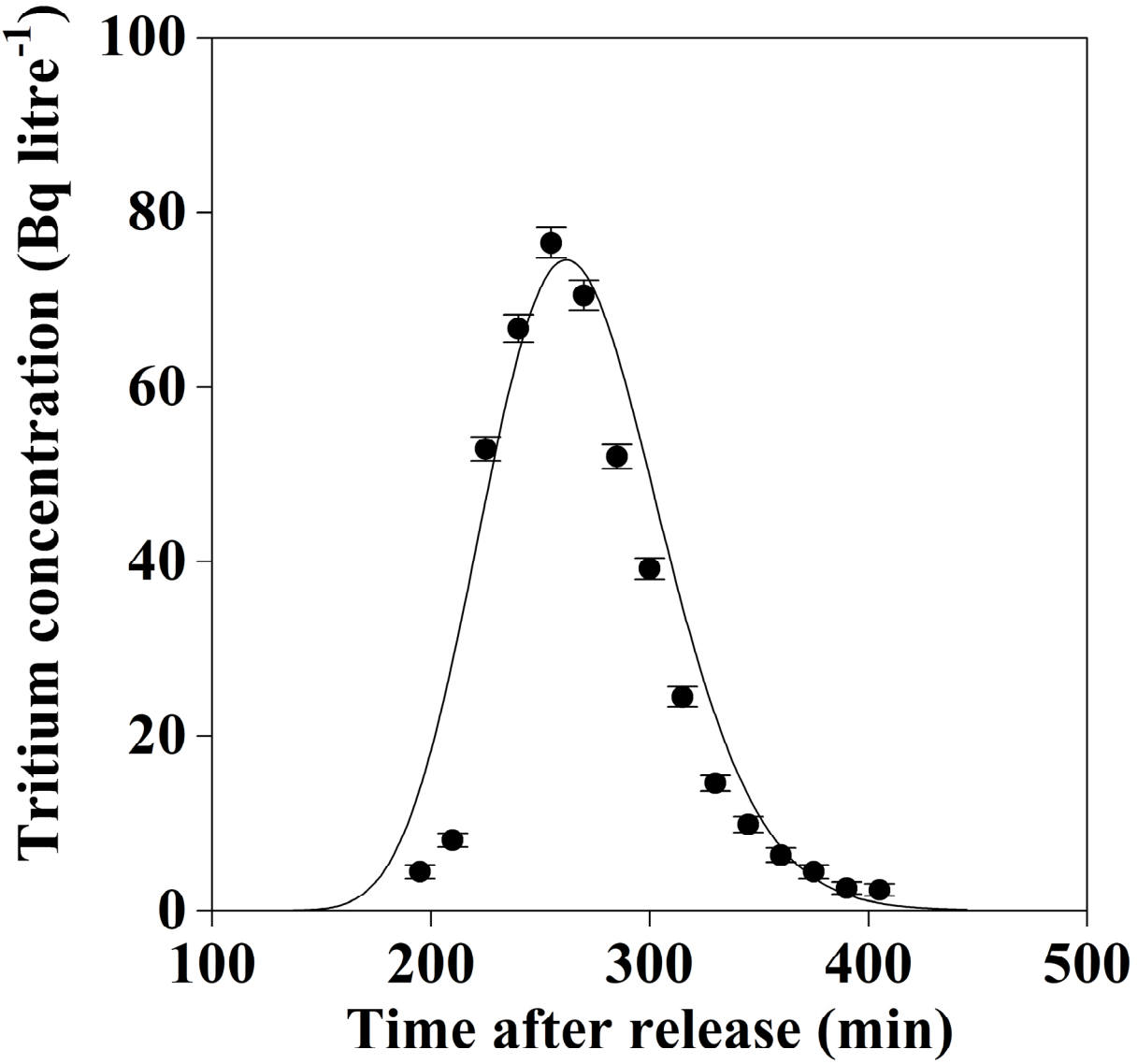

Fig. 3. Tritium concentration during the field experiment carried out at Mora de Ebro on December 5, 1991. The solid line shows the optimum box-type approach fit.

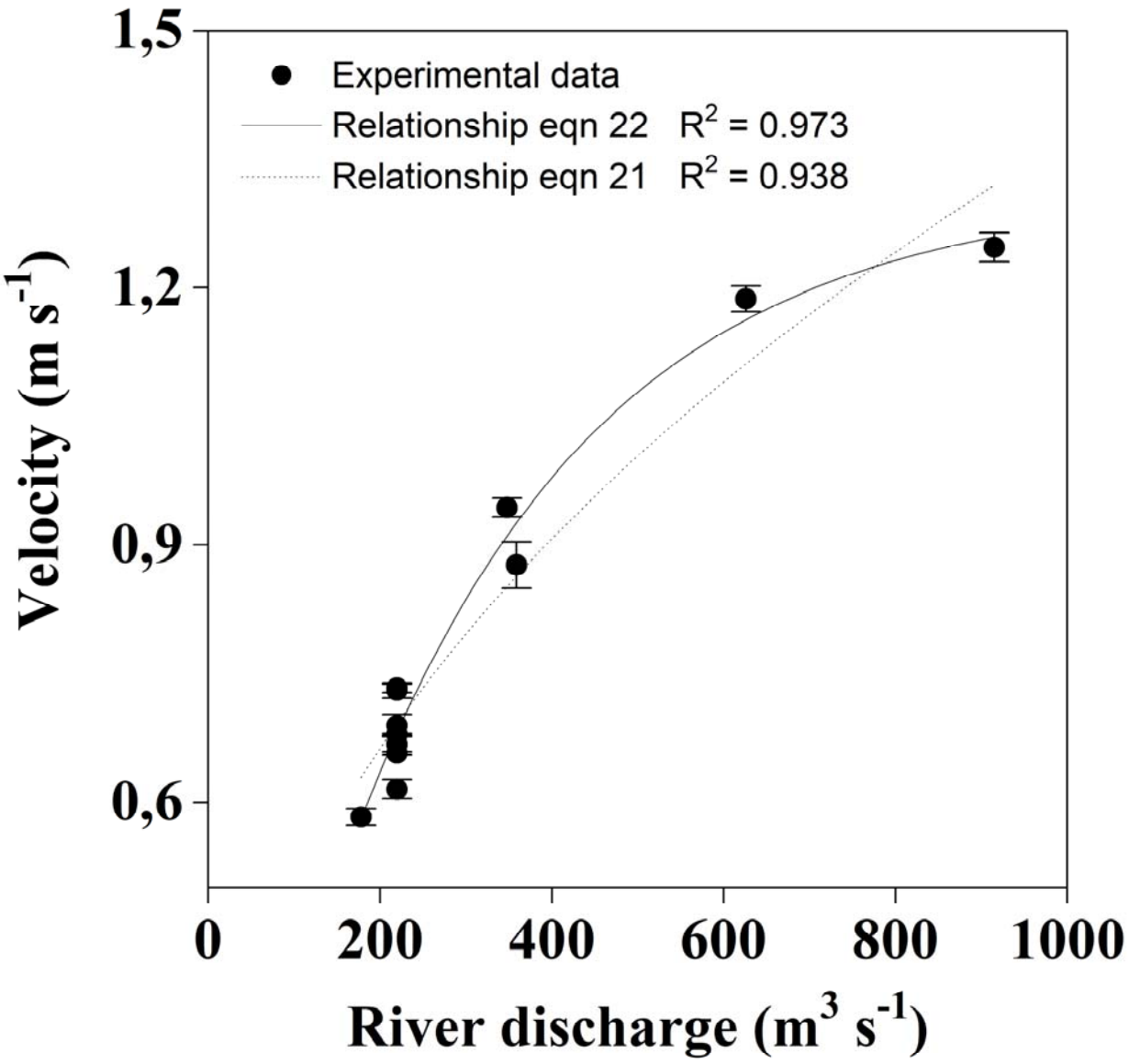

Fig. 4. Velocity as a function of river discharge for two different relationships using the analytical approach.

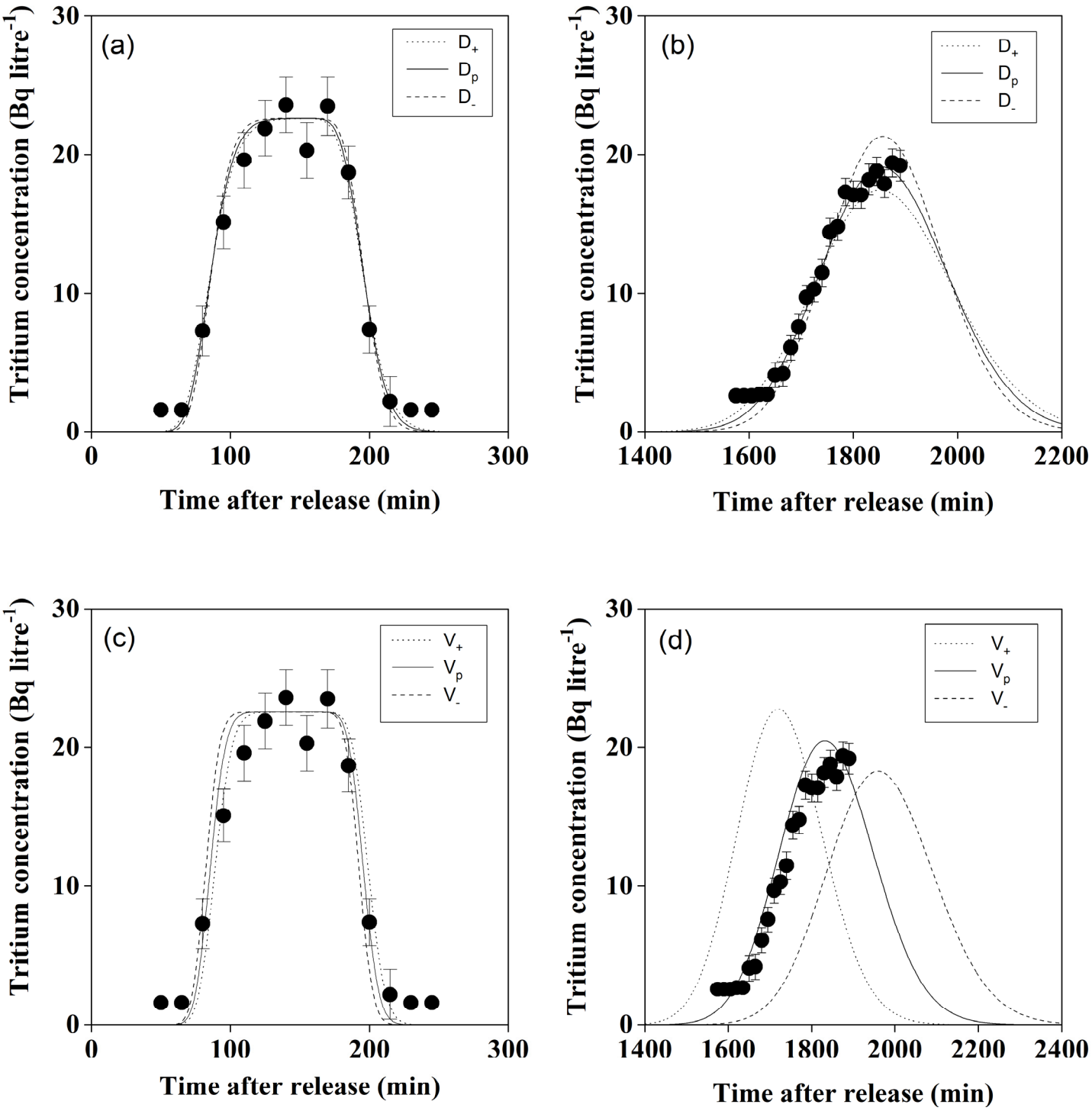

Fig. 5. Sensitivity analysis for the numerical approach. (a) Pas de l'Ase 6 May, 1991, Dp = 46 m2 s-1, D+ = 68 m2 s-1, D- = 24 m2 s-1, (b) Tortosa 20 May, 1992, Dp = 52 m2 s-1, D+ = 69 m2 s-1, D- = 35 m2 s-1, (c) Pas de l'Ase 6 May, 1991, vp = 1.26 m s-1, v+ = 1.31 m s-1, v- = 1.21 m s-1, (d) Tortosa 20 May, 1992, vp = 0.59 m s-1, v+ = 0.63 m s-1, v- = 0.55 m s-1.

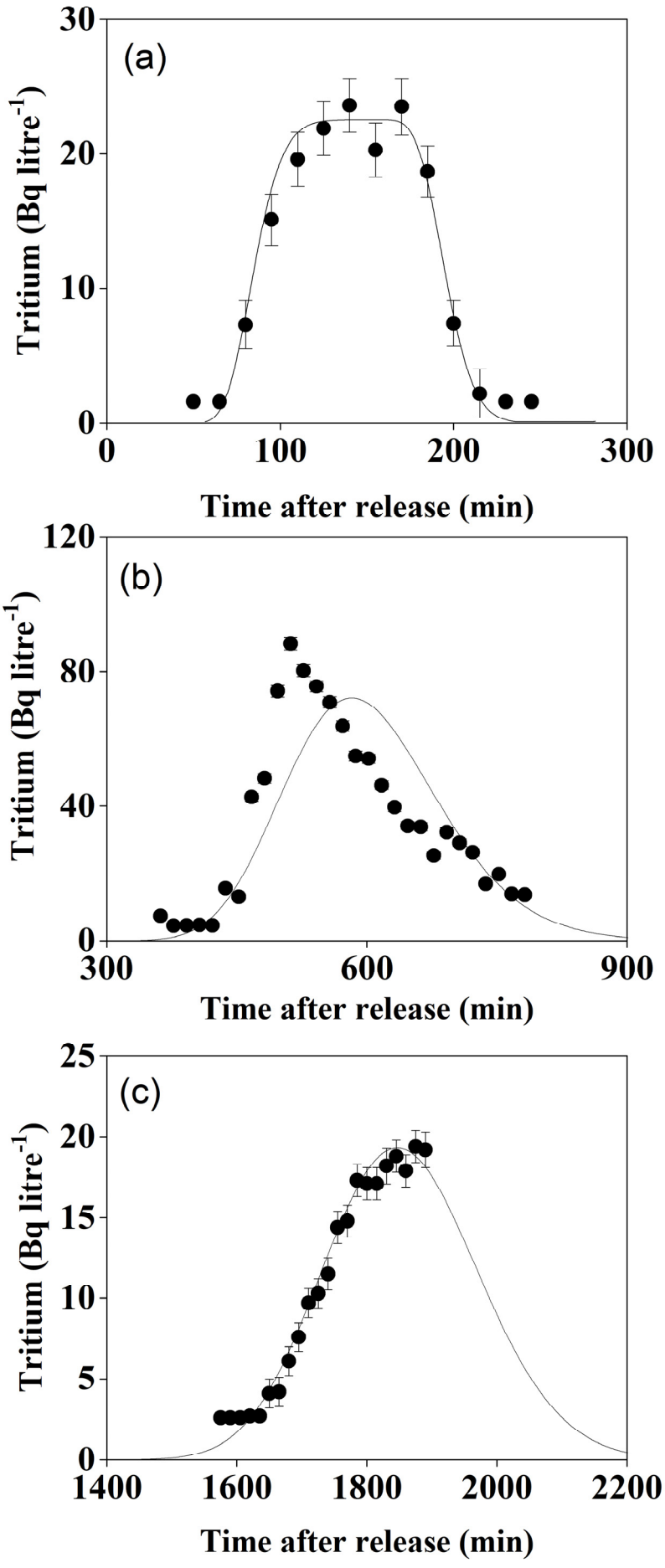

Fig. 6. Experimental data ( ) and prediction ( ) for the studied approaches. (a) numerical approach at 6.5 km from the release point in Pas de l'Ase on 6 May, 1991; (b) box-type approach at 28 km in Miravet on 16 December, 1991, (c) analytical approach at 63.5 km in Tortosa on 20 May, 1992.